ELSEVIER

Biophysical Chemistry 97 (2002) 79–86

Biophysical Chemistry

www.elsevier.com/locate/bpc

Metal ion complexation and folding of linear peptides

Ottavia Spiga[a], Maria Scarselli[a], Andrea Bernini[a], Arianna Ciutti[a], Leonardo Giovannoni[b], Franco Laschi[c], Luisa Bracci[a], Neri Niccolai[a,*]

[a]*Dipartimento di Biologia Molecolare, Centro per lo Studio Strutturale di Sistemi Biomolecolari, Via Fiorentina 1, 53100, Italy*
[b]*Dipartimento di Chimica, Università di Siena, Via Fiorentina 1, 53100, Italy*
[c]*Philogen srl Piazza La Lizza 7, 53100 Siena, Italy*

Received 21 February 2002; accepted 26 February 2002

Abstract

A Linear peptide, GASYQDLG was synthesised and used as a model to evaluate the effects of nickel additions to increase the conformational stability. The NMR data obtained for the peptide and its histidyl derivative $(H)_3$GASYQDLG$(H)_3$ suggest that in solution folded structures are present only for the H-tagged peptide-Ni(II) ion system. These results suggest that metal ions and additions of a double histidine tags of suitable length can be used as efficient tools to reduce peptide flexibility without other internal modifications. Synthesis of H-tagged analogs could offer a promising strategy for large-scale preparation of diagnostic tools and, in general, whenever more rigid molecular structures should be advisable.

Keywords: Peptide-metal complex; NMR; Nickel; Protein folding

1. Introduction

Peptide complexes with metal ions have been extensively studied in order to mimic specific metalloprotein structures and functions [1–4]. A prominent role of some amino acid side chains and, in particular, the imadazyl moieties of histidine in the binding of metal ion has been observed in proteins and in natural [5,6] or synthetic peptides [7–9]. This feature has been routinely exploited for protein purification with the insertion of histidyl tags [10].

Many structural studies indicate the atomic bases of the high affinity of histidine towards Ni(II), showing that model peptides reproducing Ni(II)-protein co-ordination sites dramatically change their conformation upon metal ion complexation [4,11,12].

In the present report, the induction of conformational changes, which can be solely ascribed to the interaction between Ni(II) and histidine residue, for linear synthetic peptides is explored.

Synthetic peptides are, indeed, good candidates for the development of new drugs and diagnostic tools, because of their favourable chemical and physical properties such as low toxicity and easy handling and storage.

*Corresponding author. Tel.: +0577-234-910; fax: +0577-234-903.

E-mail address: niccolai@unisi.it (N. Niccolai).

0301-4622/02/$ - see front matter
PII: S0301-4622(02)00041-8

Thus, the effects of the addition of N- and C-terminal histidine tags on the conformational equilibrium of the GASYQDLG octapeptide has been investigated in the presence and absence of Ni(II), in order to exploit the metal ion as a folding engine to induce a switching of the polypeptide chain from a flexible linear form to a hairpin-like conformation.

2. Materials and methods

Amino acids derivatives and the resin for the peptide synthesis were obtained from Novabiochem and all the other reagents and solvents were purchased from Applied Biosystems, Sigma, Pierce and Fluka. Solid-phase peptide synthesis was carried out on a model 350 multiple peptide synthesiser (Syro, MultiSynTech, Bochum, Germany) using standard reaction cycles with Fmoc chemistry and DIC/HOBT activation [13]. The used aminoacid side chain protecting groups were: O*t*Bu group for serine and tyrosine, Trt group for glutamine and histidine, *t*Bu group for aspartic acid. Glycine, alanine and leucine were used in an unprotected side-chain form. The Fmoc group was cleaved with a 40% (v/v) piperidine solution in DMF. The peptides were cleaved from the resin and deblocked using a cleavage cocktail consisting of 88% (v/v) TFA, 6% phenol, 2% triisopropylsilane and 4% water [13], then purified by gradient RP-HPLC on a Vydac semi-prep C18 column (1.0×25 cm). The mobile phase solvents were water containing 0.1% (v/v) TFA and methanol. A linear gradient from 0 to 100% of methanol in 30 min was applied. The yields measured by the HPLC analysis of the crude peptides were: 85% for GASYQDLG and 74% for $(H)_3$GASYQDLG$(H)_3$. Peptides identities were confirmed by amino acid analysis using PICO TAG model 510 (Waters, Milford, MA). Amino acid analysis gave $(H)_3$GASYQDLG$(H)_3$: H(6): 6.02, G(2): 2.11, A(1): 0.96, S(1): 0.85, Y(1): 1.15, Q(1): 1.00, D(1): 1.02, L(1): 0.95. Amino acid analysis gave GASYQDLG: G(2): 2.21, A(1): 0.98, S(1): 0.91, Y(1): 0.99, Q(1): 1.01, D(1): 1.06, L(1): 0.98

Both peptides, lyophilised from a pH 5.6 water solution, were dissolved in 0.5 ml of DMSO-d_6 to yield 4 mM solutions. Proton chemical shifts were referred to the solvent isotopic impurity (2.5 ppm). Additions of Ni(II) were carried out by mixing variable volumes of a 1 M solution of $NiCl_2$ in DMSO-d_6 to the peptide samples up to a molar peptide:nickel ratio of 1:5.

The structural investigation on the peptide was performed by 1D and 2D COSY, TOCSY and NOESY ^{1}H experiments. All the NMR spectra were acquired at 300 K using a Bruker DRX 600 equipped with a SGI workstation. All the data were processed and analysed with the SwaN-MR software, version 3.4.8 [14]. 1D proton NMR spectra were recorded using a spectral width of 6001.22 Hz, corresponding to 10 ppm and 32 K data points. 2D TOCSY and NOESY NMR spectra were carried out at 298 K. TOCSY experiments were employed to assign the resonances within each spin system. NOESY spectra were acquired with a mixing time of 120 ms, to detect NOE connectivities suitable for sequence specific assignment and structure determination. 2D COSY spectra, obtained in the range of 293–318 K with 5 K increments, were used to calculate the temperature coefficients of amide protons. In all the 2D spectra, a total of 512 blocks were collected in t_1 with 1024 data points and 64 scans in t_2, over a spectral width of 7 kHz. A 90-degree shifted sinebell function was applied in the t_2 dimension. The same function was imposed in t_1, on 512 points with a shift of 90 degrees. Zero filling was applied before the 2D Fourier transforming end up with a final matrix size of 2048×2048 real points. Distance restraints for structural calculation were derived from NOE intensities referring the intra-residue Hβ-Hβ correlation of the aspartyl residue to the geminal inter-proton distance of 1.7 Å. A total of 100 structures were generated using DYANA 1.5 distance geometry software [15] running on a Silicon Grafics workstation R4400, by imposing the experimental constraints. Each conformer was refined by 10 000 cycles of energy minimisation with the AMBER force field [16] following the conjugate gradient algorithm. The final mean solution structure was produced from a group of 30 refined conformers, none of which had NOE violations higher than 0.5 Å. All dis-

Table 1
Resonance assignment of the GASYQDLG peptide. ^{1}H chemical shifts (ppm), collected at 298 K

Res	NH	H_α	H_β	Others	NH $\Delta\delta/\Delta T$(ppb)
G_4	(8.47)	3.57 (3.50)			
A_5	8.54 (8.59)	4.46 (4.35)	1.20 (1.15)		6.7
S_6	8.14 (8.17)	4.28 (4.19)	3.54 (3.50–3.56)		5.4
Y_7	7.83 (7.86)	4.45 (4.34)	2.71–2.95 (2.67–2.88)	$H_{2,6}$=7.00 ($H_{2,6}$=6.97) $H_{3,5}$=6.63 ($H_{3,5}$=6.57)	4.6
Q_8	8.14 (8.06)	4.24 (4.14)	1.74–1.86 (1.68—1.80)	$CH_2\gamma$=2.08 ($CH_2\gamma$=2.06) √$H_2\delta$ 7.21–6.78 √$H_2\delta$ 7.22–6.77)	5.7
D_9	8.29 (8.21)	4.57 (4.49)	2.56–2.76 (2.51–2.69)		6.3
L_{10}	7.94 (7.89)	4.24 (4.14)	1.50–1.61 (1.43–1.54)	Hγ=1.38 (Hγ=1.40) $CH_3\delta$=0.81–0.86 ($CH_3\delta$=0.73–0.79)	7.7
G_{11}	8.01 (7.97)	3.55–3.66 (3.47–3.58)			6.5

played structures were generated with the program MOLMOL 2.5.1 software [17].

3. Results and discussion

To confirm that the origin of the peptide folding was only due to the addition of histidyl residues at the N- and C-termini, an amino acid sequence, which does not have intrinsic structural trends, was searched. Thus, GASYQDLG was selected as this octapeptide ensures a low propensity to fold in any regular conformation, as well as its H-tagged analog. For both peptides, this feature was tested on the basis of structure prediction methods [18,19] and a search among the Protein Data Bank structures [20]. Furthermore, the small molecular dimensions, the hydrophylic characters and the absence of proline residues suggested for them the commonly found unordered conformation in solution.

NMR measurements in DMSO were performed to investigate the structural properties of this peptide and the ones of its H-tagged analog $(H)_3$GASYQDLG$(H)_3$. Just during the NMR sample preparation a preliminary information on the complex formation of Ni(II) with the latter peptide could be obtained. The metal ion, indeed, gave to the DMSO solution a pale green colour, which could be attributed to the presence of residual water molecules in the organic solvent, co-ordinating Ni(II) in an octahedral complex. Also the presence of $(H)_3$DGASYQDLG$(H)_3$ in the DMSO solution determined a yellow coloured solution, which could be ascribed to the formation of a planar complex of Ni(II) with the peptide [12].

NMR spectra were recorded in DMSO-d_6, in the presence and in the absence of Ni(II) and proton chemical shifts are reported in Tables 1 and 2.

Proton NOESY spectra were recorded for each peptide at Ni(II) molar ratios of 0, 1, 2 and 5. Structurally relevant medium- and long-range Overhauser effects had been observed only for $(H)_3$GASYQDLG$(H)_3$, with intensities, which

Table 2
Resonance assignment of the $(H)_3GASYQDLG(H)_3$ peptide.[1]H chemical shifts (ppm), collected at 298 K

Res	NH	H_α	H_β	Others	NH $\Delta\delta/\Delta T$(ppb)
H_1		4.14 (4.26)	(3.21)	(H_4 = 7.41)	
H_2	8.86 (9.11)	4.64 (4.58)	2.98–3.10	(H_4 = 7.40) (H_2 = 8.95)	5.4
H_3	8.73 (8.77)	4.62 (4.56)	3.00–3.11 (3.03–3.12)	(H_4 = 7.39) (H_2 = 8.95)	5.0
G_4	8.42 (8.47)	3.73–3.85 (3.71–3.79)			5.7
A_5	8.18 (8.16)	4.38 (4.31)	1.18 (1.14)		5.5
S_6	8.05 (8.10)	4.28 (4.19)	3.53 (3.50–3.55)		5.5
Y_7	7.84 (7.86)	4.45 (4.35)	2.70–2.93 (2.66–2.87)	$H_{2,6}$ = 6.93 ($H_{2,6}$ = 6.93) $H_{3,5}$ = 6.62 ($H_{3,5}$ = 6.56)	3.3
Q_8	8.14 (8.07)	4.25 (4.16)	1.72–1.85 (1.68–1.81)	$CH_2\gamma$ = 2.09 ($CH_2\gamma$ = 2.06) $\sqrt{H_2\delta}$ 7.23–6.79 $\sqrt{H_2\delta}$ 7.24–6.76	5.5
D_9	8.25 (8.23)	4.57 (4.52)	2.52–2.72 (2.49–2.68)		5.0
L_{10}	7.84 (7.83)	4.27 (4.19)	1.45–1.61 (1.41–1.84)	$H\gamma$ = 1.45 ($H\gamma$ = 1.41) $H_3\delta$ = 0.80–0.85 ($CH_3\delta$ = 0.75–0.78)	5.2
G_{11}	8.14 (8.17)	3.69 (3.67)			5.5
H_{12}	8.14 (8.24)	4.56 (4.52) (2.91–3.07)	2.91–3.06 (H_4 = 7.25)	H_4 = 7.26	5.4
H_{13}	8.32 (8.48)	4.55 (4.54)	2.93–3.12 (2.99–3.10)	H_4 = 7.29	5.3
H_{14}	8.34 (8.45)	4.49 (4.47)	2.98–3.11 (2.99–3.10)		5.7

reached a maximum at the highest metal ion concentration. For this reason, all NOE data discussed below and shown in Fig. 1 were collected in the presence of 20 mM Ni(II). It should be noted that this feature implies a rather weak complexation of Ni(II) from both peptides in the DMSO solution. However, the appearance of new NOEs upon addition of the metal ion is diagnostic of an Ni(II)-induced peptide folding.

This is not the case of the GASYQDLG peptide, as its NOESY spectra are characterised only by the presence of strong intra-residue and (i, $i+1$) sequential correlations, either in presence and absence of Ni(II), indicating that it does not assume any particular conformation in solution. Furthermore, the temperature coefficients of proton chemical shifts (see Tables 1 and 2), do not suggest a finite hydrogen-bonding pattern, consistent with a single and stable peptide conformation.

However, a structural order, induced by the metal ion in the histidine-containing peptide, is apparent. Although the strong sequential NOEs are still present, upon the addition of Ni(II), $(H)_3GASYQDLG(H)_3$ exhibits a set of new NOEs, most of them involving side chain protons (Table 3 and Fig. 2d) in addition to some (i, $i+2$) and (i, $i+3$) backbone correlations (Fig. 3). These findings suggest a more restricted conformational space for the histidyl-tagged peptide and a pronounced bending of the main chain in the

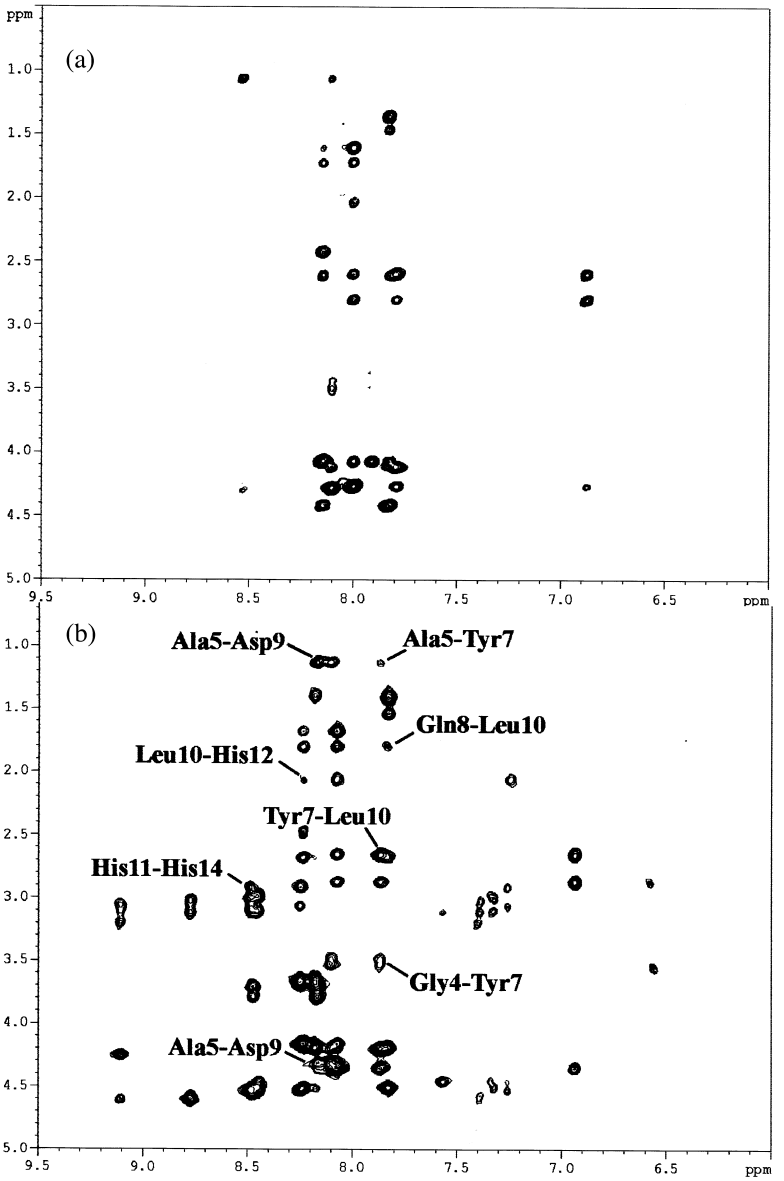

Fig. 1. Fingerprint regions of the ^{1}H 600 MHz NOESY spectra of 4 mM $(H)_3$GASYQDLG$(H)_3$ recorded at 298 K (a) in the absence and (b) in the presence of 20 mM Ni(II) ion. Some of the NOE, which are detectable only upon the addition of the metal ion, are highlighted.

ASYQD portion of the molecule. The many dipolar connectivities found among histidyl Hβ and H4 protons, see the insets in Fig. 1b, no use was made of this information due to severe spectral overlapping among the six H residues, which prevents a rigorous assignment and integration of these NOESY cross-peaks.

A panel of 131 NOEs, derived from the analysis of the NOESY map of $(H)_3$GASYQDLG$(H)_3$, was used as distance constraint in a molecular

Table 3
List of the conformationally relevant NOEs appearing only upon the addition of Ni(II) to the $(H)_3$GASYQDLG$(H)_3$ peptide sample. Asterisks are placed where pseudo-atoms were used

Intra-residue	$i, i+1$	$i, i+2$	$i, i+3$	$i, i+4$
$H\beta_2$(His1)-Hα(His1)	Hα(His3)-Hα_1(Gly4)	Hβ_2 (His1)-Hβ*(His3)	Hα_1 (Gly4)-HN(Tyr7)	Hα_1 (Ala5)-HN(Asp9)
	Hα_1(Gly4)-Hα(Ala5)	Hα (His3)-HN(Ala5)	Hα_1 (Gly4)-Hβ*(Tyr7)	$CH_3\beta$(Ala5)-HN(Asp9)
	Hα_1(Gly4)-$CH_3\beta$(Ala5)	HN(Gly4)-HN(Ser6)	$CH_3\beta$(Ala5)-Hα(Gln8)	
	Hα_2(G1y4)-$CH_3\beta$(Ala5)	$CH_3\beta$ (Ala5)-HN(Tyr7)	Hβ*(Tyr7)-HN(Leu10)	
	Hα_1(Gly4)-HN(Ser6)	HN(Ala5)-HN(Tyr7)	Hδ1 (Tyr7)-Hβ_2 (Leu10)	
	HN(Tyr7)-Hβ_2(Gln8)	Hβ_2(Gln8)-Hβ_2(Leu10)	Hδ1(Tyr7)-Hδ2(Leu10)	
	HN(Tyr7)-Hβ_1(Gln8)	Hβ_2(Gln8)-Hδ2 (Leu10)	Hδ2(Tyr7)-Hδ2(Leu10)	
	Hα(Tyr7)-Hβ_1(Gln8)	Hβ*(Gln8)-HN(Leu10)	Hδ1 (Leu 10)-Hα (His13)	
	HN(Gln8)-Hα(Asp9)	Hβ*(Gln8)-Hδ2(Leu10)	Hδ2(Leu 10)-Hα(His13)	
	HN(Leu10)-Hα_1(Gly11)	Hβ_2(Leu10)-Hα(His12)	Hβ_2 (His11)-HN(His14)	
	Hβ_2(His11)-HN(His14)	Hβ_2(Leu10)-HN(His12)		
		Hβ*(Leu10)-HN(His12)		
		Hδ_1(Leu10)-Hα(His12)		
		Hδ_2(Leu10)-Hα(His12)		

dynamics calculation to elucidate the peptide structure. Among them, 40 were $(i, i+1)$ distances, 17 $(i, i+2)$, 8 $(i, i+3)$, and 2 $(i, i+4)$.

In the 30 conformers with the lowest overall energy, none of these structures had distance violations greater than 0.54 Å and the total r.m.s.d. calculated for backbone heavy atoms was 0.38 Å, suggesting a rather rigid structure for such molecular moiety.

The lack of a large number of NOE restraints at both amino and carboxyl termini, due to the local signal overlap, prevents a detailed structural analysis of the Ni(II) complex geometry. However, the observation that, under our experimental conditions, a diamagnetic complex is obtained, indicates the low-spin character of the Ni(II) which adopts a square planar geometry, consistent with the 4N co-ordination of the metal ion [4,21]. On the basis of this consideration and the obtained

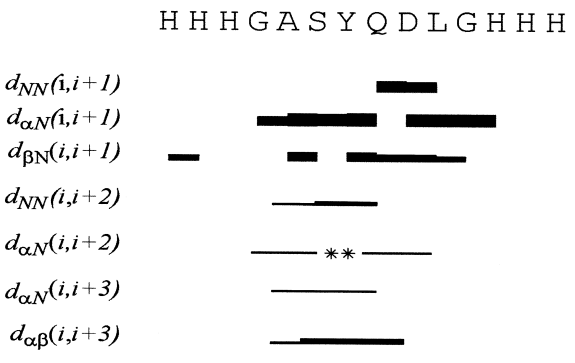

Fig. 2. Panel of the NOE connectivities diagnostic for secondary structure observed for $(H)_3$GASYQDLG$(H)_3$ in DMSO-d_6 solution in the presence and in the absence of Ni(II). Intervening NOE effects upon the ion addition are reported in black; intensities are reflected by the thickness of lines. Asterisks mark the NOE whose presence is clearly detected but not translated in distance restraints due to spectral overlapping.

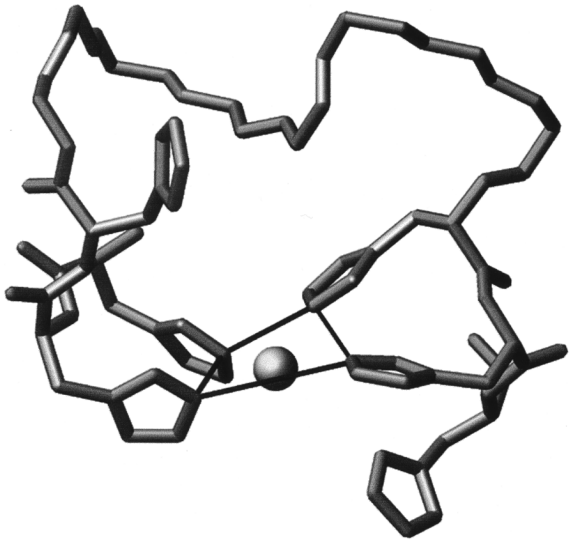

Fig. 3. Backbone representation of the lowest energy structure of $(H)_3$GASYQDLG$(H)_3$. Only the histidyl side chains, oriented as described in the text, are shown.

backbone conformation, only few orientations of the histidyl side chains can be found in agreement with the metal ion planar co-ordination and the one exhibiting the lowest energy is shown in Fig. 3.

Our data can be summarised in the following way: (a) extensive conformational equilibrium may be suggested for GASYQDLG and $(H)_3$GASYQDLG$(H)_3$ in the absence of the metal ion, as largely predictable for linear peptides of this length; (b) no structural order was induced by Ni(II) in the absence of any histidyl residues, since in this case no detectable medium and long-range NOE for GASYQDLG could be observed. The possibility of a stable ion complex with the aspartyl and tyrosyl side chains, as well as to backbone carboxyl groups, which have been demonstrated to be potential donors in Ni(II)-peptides interaction studies [21], for both peptides can be ruled out; (c) the conformation of the H-tagged peptide is totally influenced by the Ni(II) complex formation.

These data suggest that Ni(II) chelation can be used to mildly constraint very flexible peptides enhancing biological properties such as the immuno-chemical reactivity, particularly advisable for the development of diagnostic tools.

Acknowledgments

NN and LB thank the Italian C.N.R. (Progetto Finalizzato Biotecnologie), MURST (PRIN99) and the University of Siena for financial supports.

References

[1] L. Regan, Protein design: Novel metal-binding sites, TIBS Rev. 20 (1995) 280–285.

[2] W. Bal, J. Lukszo, K.S. Kasprazak, Interactions of nickel(II) with histones: enhancement of T-deoxyguanosine oxidation by Ni(II) complexes with CH_3CO-Cys-Ala-Ile-His-NH_2, a putative metal binding sequence of histone H_3, Chem. Res. Toxicol. 9 (2) (1996) 535–540.

[3] G. Xing, V.J. DeRose, Related articles designing metal-peptide models for protein structure and function, Curr. Opin. Chem. Biol. Rev. 5 (2) (2001) 196–200.

[4] Y. Lu, S.M. Berry, T.D. Pfister, Engineering Novel Metalloproteins: Design of Metal-Binding Sites into Native Protein Scaffolds Chem. Rev., 101 (10), 3047–3080, (2001), Curr. Opin. Chem. Biol. Rev. 2 (2001) 196–200.

[5] M.A. Zoroddu, T. Kowalik-Jankowska, H. Kozlowsky, et al., Interaction of Ni(II) and Cu(II) with a metal binding sequence of histone H4: AKRHRK, a model of the H_4 tail, Biochim. Biophys. Acta 1475 (2000) 163–168.

[6] G.J. Colpas, T.G. Brayman, L.J. Ming, R.P. Hausinger, Identification of metal-binding residues in the Klebsiella aerogenes urease nickel metallochaperone, UreE Biochem. 38 (13) (1999) 4078–4088.

[7] P. Tsiveriotis, N. Hadjiliadis, Studies the interaction of histidyl containing peptides with palladium(II) and platinum(II) complex ions, Co-ordination Chem. Rev. 190–192 (1999) 171–184.

[8] W. Bal, Axial hydrophobic fence in higly-stable Ni(II) complex of desangiotensinogen N-terminal peptide, J. Am. Chem. Soc. 118 (1996) 4727–4728.

[9] P. Mlyanrz, W. Bal, U. Kowalik, et al., Introduction of alpha-hydroxymethylserine residues in a peptide sequence results in the strongest peptidic, albumin-like, copper(II) chelator known to date, J. Chem. Soc. Dalton Trans. 2 (1999) 109–110.

[10] K.M. Muller, K.M. Arndt, K. Bauer, A. Plückthun, Tandem immobilised metal-ion affinity chromatography/immunoaffinity purification of his-tagged proteins evaluation of two Anti-His-Tag monoclonal antibodies, Anal. Biochem. 259 (1998) 54–61.

[11] W. Bal, M. Jerzowka-Bojczuk, K.S. Kasprzak, Ni(II) specifically cleaves the C-terminal tail of the major variant of histone H_2A and forms an oxidative damage-mediating complex with the cleaved-off octapeptide, Chem. Res. Toxicol. 10 (1997) 906–914.

[12] G. Gasmi, A. Singer, J. Forman-Kay, B. Sarkar, NMR structure of neuromedin C, a neurotrasmitter with an amino terminal CuII, NiII-binding (ATCUN) motif, J. Peptide Res. 49 (1997) 500–509.

[13] W. Koning, R. Geiger, A new method for the synthesis of peptides: activation of the carboxy group with dicyclohexylcarbadiiamide and 3-hydroxy-4-oxo-3,4-dihydro-1,2,3-benzotriazine, Chem Ber. 103 (788) (1970) 2024–2034.

[14] G. Balacco, SwaN-MR: A complete and expansible NMR software for the Macintosh, J. Chem. Inf. Comput. Sci. 34 (1994) 1235–1241.

[15] P. Guntert, C. Mumenthaler, K. Wüthrich, Torsion angle dynamics for NMR structure calculation with the new program DYANA, J. Mol. Biol. 273 (1997) 283–298.

[16] W.D. Connell, P. Cieplak, C.I. Bayly, et al., A second-generation force field for the simulation of proteins, nucleic acids and organic molecules, J.A.C.S. 117 (1995) 5179–5197.

[17] R. Koradi, M. Billeter, K. Wüthrich, MOLMOL: a program for display and analysis of macromolecular structures, J. Mol. Graphics 14 (1996) 51–55.

[18] http://www.sdsc.edu/ResTools/biotools/biotools9.html
[19] http://bmerc-www.bu.edu/psa/
[20] H.M. Berman, J. Westbrook, Z. Feng, et al., The protein data bank, Nucleic Acids Res. 28 (2000) 235–242.
[21] M.A. Zoroddu, T. Kowalik-Jankowska, H. Kozlowski, K. Salnikow, M. Costa, Ni(II) and Cu(II) binding with a 14-aminoacid sequence of Cap43 protein, TRSRSHTSEGTRSR, J. Inorg. Biochem. 84 (2001) 47–54.